Adsorption of Water at the SrO Surface of Ruthenates

Daniel Halwidl[1,+], Bernhard Stöger[1,+], Wernfried Mayr-Schmölzer[1,2], Jiri Pavelec[1], David Fobes[3], Jin Peng[3], Zhiqiang Mao[3], Gareth S. Parkinson[1], Michael Schmid[1], Florian Mittendorfer[1,2], Josef Redinger[1,2], and Ulrike Diebold[1,*]

[1]Institute of Applied Physics, TU Wien, Wiedner Hauptstrasse 8-10/134, A-1040 Vienna, Austria
[2]Center for Computational Materials Science, TU Wien, Wiedner Hauptstrasse 8-10/134, A-1040 Vienna, Austria
[3]Department of Physics and Engineering Physics, Tulane University, New Orleans, LA 70118, USA

Supplementary Information

1 Activation energy measurement

The hopping of the OH_{ads} group was modelled as one-dimensional, thermally activated random walk [1]. Therefore the hopping rate R (i.e. the reciprocal average lifetime τ^{-1}) varies with absolute temperature T as

$$R = \tau^{-1} = \nu \exp\left(-\frac{E_{\text{act}}}{kT}\right), \tag{S1}$$

where ν is an attempt frequency and E_{act} is the activation energy. To obtain the activation energy, we measured the average lifetime τ at different temperatures by analyzing consecutive frames of STM movies.

To motivate our analysis method, we note that for constant temperature the hopping rate is a constant and that the occurrence of a next hop is independent from the last hop, qualifying the hopping as a Poisson process. Therefore the lifetimes t_i of the OH_{ads} group are exponentially distributed according to

$$N(t_i) \propto \exp\left(-\frac{t_i}{\tau}\right). \tag{S2}$$

+ These authors contributed equally to the work
* Corresponding author: diebold@iap.tuwien.ac.at

Determining the lifetime distribution $N(t_i)$ from the STM movie and fitting to Eq. (S2) gives the average lifetime for the particular temperature. When the count of lifetimes was too small (<100) for a reasonable fit, the hopping rate was calculated according to

$$R = \tau^{-1} = \frac{1}{t_\mathrm{f}} \frac{\sum_{j=1}^{n-1} m_j}{\sum_{j=1}^{n-1} a_j}\,, \tag{S3}$$

where a_j is the number of evaluated OH_{ads} groups in frame j, m_j is the number of observed hops between frame j and $j+1$, t_f is the acquisition time for a single frame and n ist the total number of frames. The standard error of the hopping rate is then given as

$$\sigma_R = \frac{1}{t_\mathrm{f}} \frac{\sqrt{\sum_{j=1}^{n-1} m_j}}{\sum_{j=1}^{n-1} a_j}\,. \tag{S4}$$

1.1 Experimental procedure

The Sr_2RuO_4 sample was cleaved at 107 K in the analysis chamber as described in [2] and transferred to the cold STM (78 K) to confirm the surface cleanliness. Then the sample was transferred on a cold manipulator (110 K) to the preparation chamber where 0.01 L H_2O were dosed ($p_{H_2O} = 1.0 \times 10^{-10}$ mbar for 133 s). The sample was transferred back to the STM.

For the STM movies the temperature of the cryostat of the STM was lowered by evacuating the volume above the LN_2 by a roughing pump. Constant pumping decreased the temperature of the cryostat to 53 K within 12 hours. After the pumping was switched off (with the pumped volume kept sealed) the temperature increased slowly with an approximate rate of 0.5 K/h. Decoupling the STM head from the cryostat sufficiently slowed the rate of temperature change at the STM head to approximately 0.2 K/h during the recording of the movies. The mean of the temperatures at the start and the end of the STM movie was taken as temperature for the measured hopping rate. The acquisition time of one STM image was chosen sufficiently fast so that no double hops between two consecutive images were observed. All STM images were recorded with 0.1 nA tunnelling current and + 0.2 V bias. Supplementary Movies 4-8 were recorded with an unusual tip condition that show the usually bright OH_{ads} groups as dark features.

1.2 Analysis

Supplementary Table 1 shows the acquisition details of the recorded movies and the resulting average lifetimes. Supplementary Movies 1 and 2 were analyzed

Supplementary Movie	T [K]	frames	t_f [s]	lifetimes	τ [s]	σ_τ [s]
1	65.6	40	67.5	8	2605.5	476.1
2	67.3	66	100.0	69	1344.8	130.2
3	69.15	70	100.0	210	460.0	51.2
4	71.0	35	60.0	241	147.7	5.2
5	72.7	63	40.0	305	94.7	5.7
6	75.55	98	21.4	437	30.0	0.5

Supplementary Table 1 | Acquisition details of the movies and measured average lifetimes. Mean temperature T, number of recorded frames, acquisition time per frame t_f, count of lifetimes, average lifetime τ and standard error σ_τ.

Supplementary Movie	T [K]	frames	t_f [s]	lifetimes	τ [s]	σ_τ [s]
4	71.0	35	60.0	241	191.7	11.1
7	71.15	16	48.0	29	198.0	37.2
8	71.25	30	33.1	21	213.3	50.8

Supplementary Table 2 | Acquisition details and measured average lifetimes of Supplementary Movie 4 and the additional Supplementary Movies 7 and 8, recorded at 71.0 K. Supplementary Movies 7 and 8 were analyzed according to Eq. (S3) due to the small count of lifetimes. To provide comparability the same equation was used for Supplementary Movie 4.

according to Eq. (S3) because of the low count of lifetimes. Supplementary Movies 3-6 were analyzed according to Eq. (S2). OH_{ads} groups adsorbed next to a surface defect or close to another OH_{ads} group were ignored in the analysis.

Two additional STM movies at 71.0 K with different intervals between frames were recorded (Supplementary Movies 7 and 8). No tip-induced hopping was found as the measured average lifetimes are in good agreement with each other, see Supplementary Table 2.

1.3 Arrhenius equation

In Fig. 2d we plot $\ln \tau^{-1}$ vs $1000/T$ and fit the Arrhenius equation (logarithm of Eq. (S1))

$$\ln \tau^{-1} = \ln \nu - \frac{E_\mathrm{act}}{kT} \,. \tag{S5}$$

The fit gives the activation energy and the attempt frequency:

$$E_\mathrm{act} = 187 \pm 10\,\mathrm{meV} \quad \text{and} \quad \nu = 10^{(11.0\pm0.7)}\,\mathrm{s}^{-1} \,.$$

Supplementary Movie	T_{start} [K]	T_{end} [K]	recording time [min]
1	65.7	65.5	45
2	67.1	67.5	110
3	68.9	69.4	117
4	70.9	71.1	35
5	72.6	72.8	42
6	75.5	75.6	35
7	71.1	71.2	12
8	71.2	71.3	16

Supplementary Table 3 | Additional movie acquisition details. Temperatures at the start and at the end, and recording time of the movies.

2 Supplementary Movie captions

Supplementary Movie 1 Time-lapse STM movie recorded at 65.6 K (frame size $20.0 \times 20.0\,\mathrm{nm}^2$, $V_{\mathrm{sample}} = +0.2\,\mathrm{V}$, $I_{\mathrm{tunnel}} = 0.1\,\mathrm{nA}$).

Supplementary Movie 2 Time-lapse STM movie recorded at 67.3 K (frame size $20.0 \times 20.0\,\mathrm{nm}^2$, $V_{\mathrm{sample}} = +0.2\,\mathrm{V}$, $I_{\mathrm{tunnel}} = 0.1\,\mathrm{nA}$).

Supplementary Movie 3 Time-lapse STM movie recorded at 69.15 K (frame size $20.0 \times 20.0\,\mathrm{nm}^2$, $V_{\mathrm{sample}} = +0.2\,\mathrm{V}$, $I_{\mathrm{tunnel}} = 0.1\,\mathrm{nA}$).

Supplementary Movie 4 Time-lapse STM movie recorded at 71.0 K (frame size $20.0 \times 20.0\,\mathrm{nm}^2$, $V_{\mathrm{sample}} = +0.2\,\mathrm{V}$, $I_{\mathrm{tunnel}} = 0.1\,\mathrm{nA}$). An unusual tip condition shows the usually bright $\mathrm{OH}_{\mathrm{ads}}$ groups as dark features.

Supplementary Movie 5 Time-lapse STM movie recorded at 72.7 K (frame size $15.0 \times 15.0\,\mathrm{nm}^2$, $V_{\mathrm{sample}} = +0.2\,\mathrm{V}$, $I_{\mathrm{tunnel}} = 0.1\,\mathrm{nA}$). An unusual tip condition shows the usually bright $\mathrm{OH}_{\mathrm{ads}}$ groups as dark features.

Supplementary Movie 6 Time-lapse STM movie recorded at 75.55 K (frame size $15.0 \times 15.0\,\mathrm{nm}^2$, $V_{\mathrm{sample}} = +0.2\,\mathrm{V}$, $I_{\mathrm{tunnel}} = 0.1\,\mathrm{nA}$). An unusual tip condition shows the usually bright $\mathrm{OH}_{\mathrm{ads}}$ groups as dark features.

Supplementary Movie 7 Time-lapse STM movie recorded at 71.15 K (frame size $15.0 \times 15.0\,\mathrm{nm}^2$, $V_{\mathrm{sample}} = +0.2\,\mathrm{V}$, $I_{\mathrm{tunnel}} = 0.1\,\mathrm{nA}$). An unusual tip condition shows the usually bright $\mathrm{OH}_{\mathrm{ads}}$ groups as dark features.

Supplementary Movie 8 Time-lapse STM movie recorded at 71.25 K (frame size $10.0 \times 10.0\,\mathrm{nm}^2$, $V_{\mathrm{sample}} = +0.2\,\mathrm{V}$, $I_{\mathrm{tunnel}} = 0.1\,\mathrm{nA}$). An unusual tip condition shows the usually bright $\mathrm{OH}_{\mathrm{ads}}$ groups as dark features.

3 Supplementary Figures

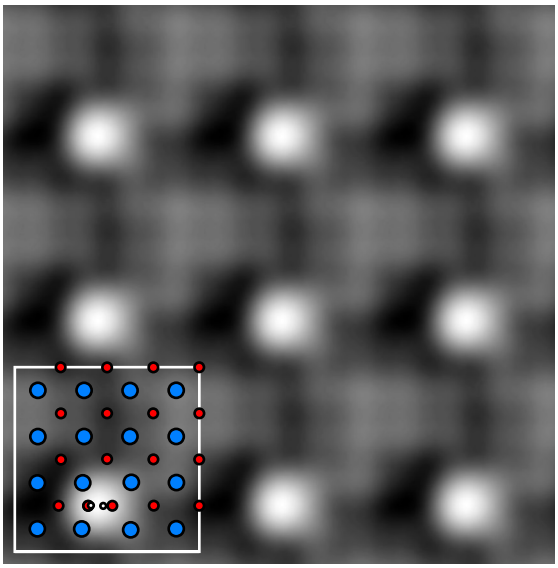

Supplementary Figure 1 | Tersoff-Haman STM simulation of a dissociated water molecule on $Sr_3Ru_2O_7$. States up to 200 meV above E_{Fermi} are shown. The real space structure is shown in the inset (blue - Sr, red - O, white - H).

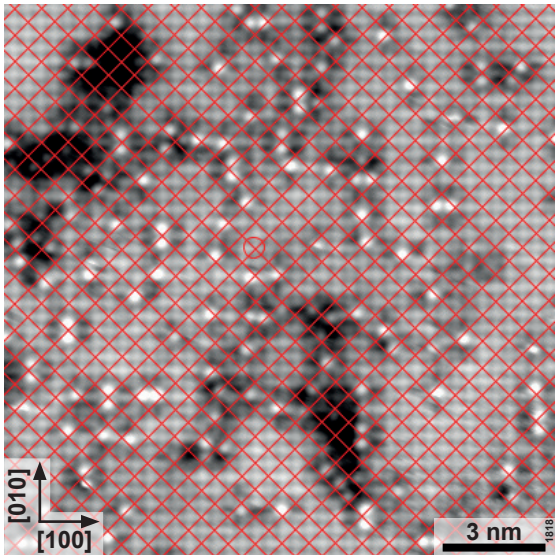

Supplementary Figure 2 | Small amount of water adsorbed on Sr_2RuO_4. STM image of Sr_2RuO_4 after dosing 0.05 Langmuir H_2O at 115 K ($T = 78\,K$, $V_{sample} = +0.05\,V$, $I_{tunnel} = 0.15\,nA$, image rotated 21° clockwise to scan direction). The overlayed grid represents the $c(2 \times 2)$ unit cell. Horizontally [100]/vertically [010] orientated dimers sit in the center/at the corner of the $c(2 \times 2)$ unit cell.

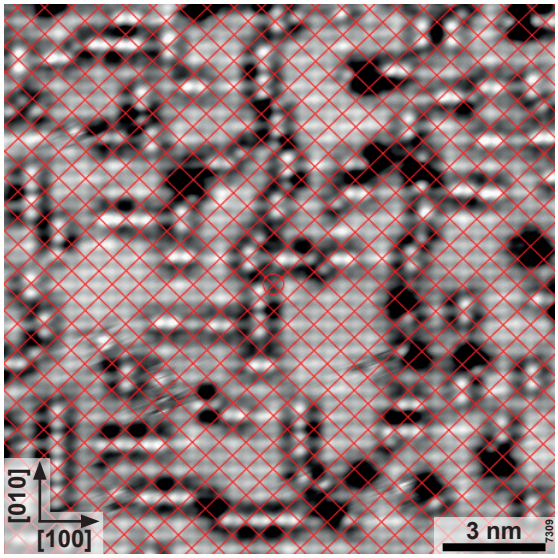

Supplementary Figure 3 | Small amount of water adsorbed on $Sr_3Ru_2O_7$. STM image of $Sr_3Ru_2O_7$ after annealing a H_2O dose of 0.05 Langmuir to room temperature for 1 hour ($T = 78\,K$, $V_{sample} = +0.5\,V$, $I_{tunnel} = 0.15\,nA$, image rotated 20° counterclockwise to scan direction). The overlayed grid represents the $c(2 \times 2)$ unit cell. Horizontally [100]/vertically [010] orientated dimers sit in the center/at the corner of the $c(2 \times 2)$ unit cell.

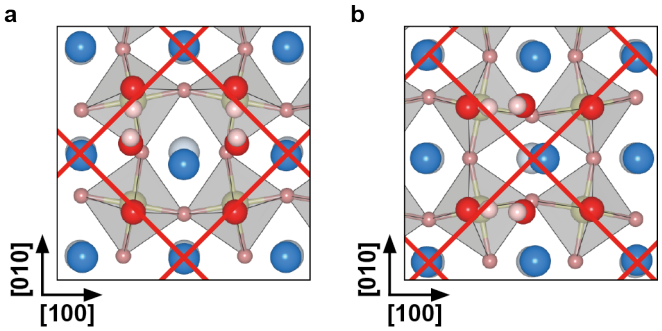

Supplementary Figure 4 | Preferred position of the dimer with respect to the $c(2 \times 2)$ unit cell. Dimer sitting along the (a) [100], (b) [010] direction.

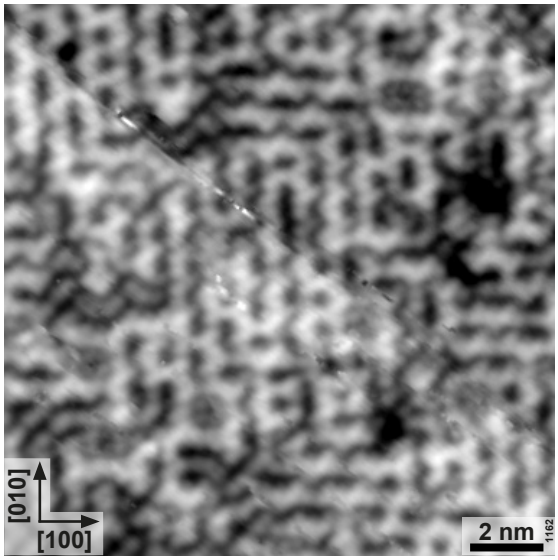

Supplementary Figure 5 | Water overlayer on $Sr_3Ru_2O_7$. STM image of $Sr_3Ru_2O_7$ after dosing 1.0 Langmuir H_2O at 160 K ($T = 78$ K, $V_{\text{sample}} = +0.5$ V, $I_{\text{tunnel}} = 0.15$ nA, image rotated 39° clockwise to scan direction).

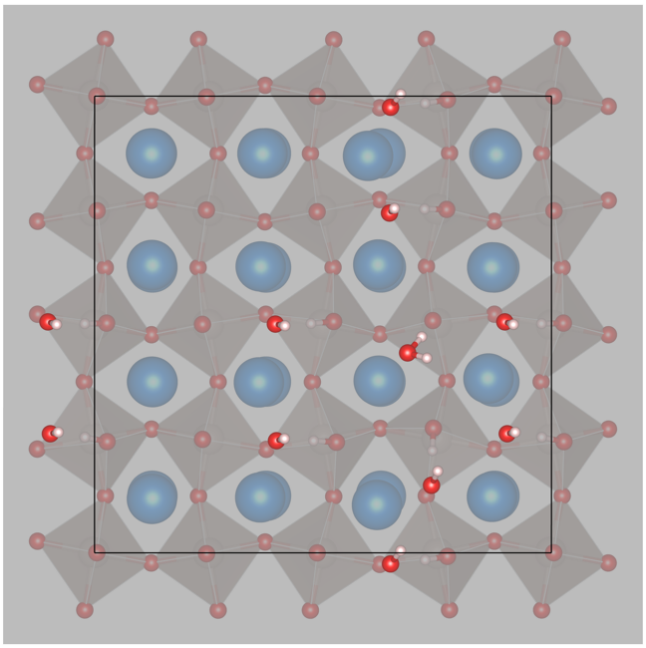

Supplementary Figure 6 | Structural model for the high-coverage adsorption of H_2O at the Sr_2RuO_4 surface.

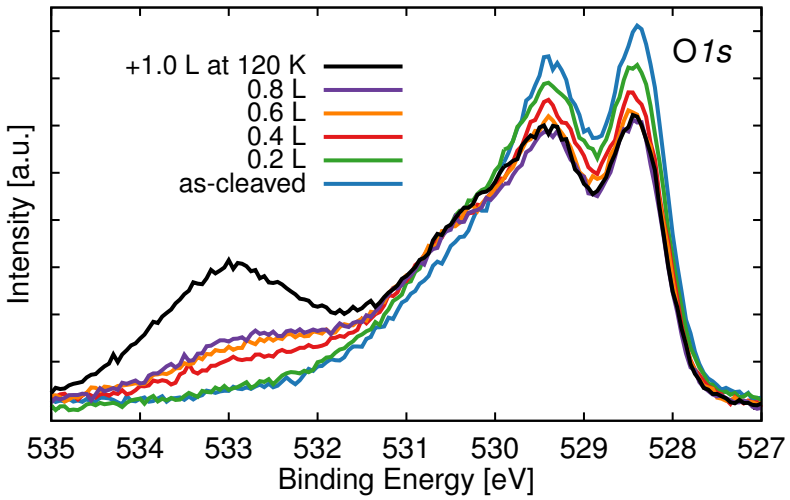

Supplementary Figure 7 | XPS spectra of the O*1s* region after exposure of the clean, cleaved Sr_2RuO_4 surface to increasing doses of water at 140 K. The shoulder and peaks at 530.4 eV, 532.8 eV and 533.1 eV are indicative of hydroxyls, molecular water and multilayer water, respectively.

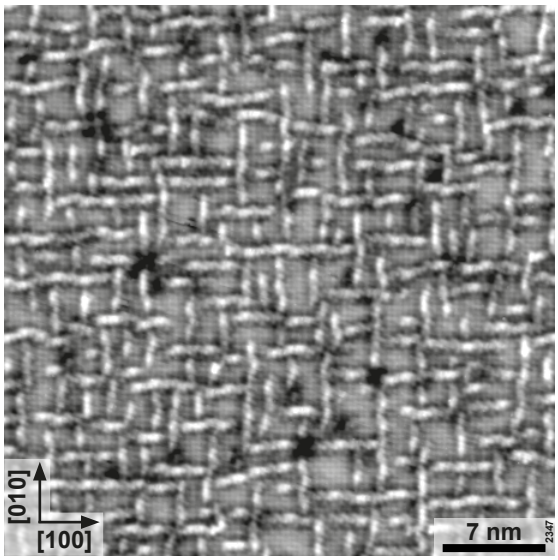

Supplementary Figure 8 | Water chains on Sr_2RuO_4 after annealing to room temperature. STM image of Sr_2RuO_4 after dosing 1.0 Langmuir H_2O at 155 K and annealing to room temperature for 17 hours ($T = 78$ K, $V_{\text{sample}} = +0.6$ V, $I_{\text{tunnel}} = 0.1$ nA, image rotated 17° clockwise to scan direction). Most of the water has desorbed, only a network of chains remains on the surface.

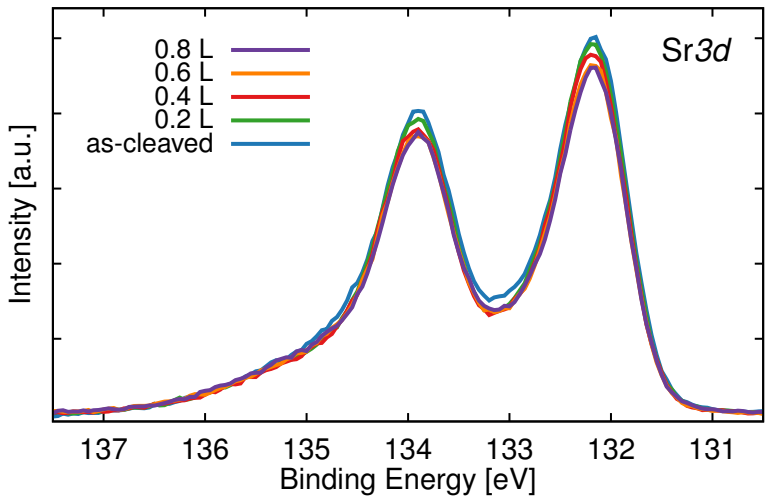

Supplementary Figure 9 | XPS spectra of the Sr*3d* region. The clean, cleaved Sr_2RuO_4 surface is exposed to increasing doses of water at 140 K.

4 XPS measurements

The samples were glued on Ta plates that were mounted to the end of a LHe cryostat. The stated temperatures were measured by a diode inside the cryostat, hence the real temperature at the samples was higher. Temperature was controlled by a resistive heater inside the cryostat. The samples were exposed to water by background dosing to the chamber, where 0.1 L (Langmuir) equals 5.0×10^{-10} mbar for 266 s.

Dose values only refer to the integrated pressure over the times when the leak valve was open, not taking into account any H_2O adsorption from the water in the residual gas ($p_{H_2O} \approx 7.0 \times 10^{-11}$ mbar) during the remaining time. Thus, the actual H_2O doses were higher.

Supplementary Figure 7 shows the O*1s* region after exposure of the clean, cleaved Sr_2RuO_4 surface to increasing doses of water at 140 K. The as-cleaved spectrum shows a two-peak structure with peaks at 528.4 eV and 529.4 eV. These energies correspond to the position of the maxima of the peaks as no conclusive fit parameters were found for the asymmetric peak shapes. Dosing 0.2 L leads to a shoulder at 530.4 eV, indicative of OH. The peak position was determined by subtracting the as-cleaved spectrum from the 0.2 L spectrum. Note that already in the as-cleaved spectrum a small contribution of OH can be seen, which presumably originated from the water in the residual gas and the time (30 minutes) between cleaving and recording the first XPS spectrum. Dosing another 0.2 L leads to a peak at 532.8 eV, indicative of molecular water, which saturates at 0.8 L. The peak position was determined by subtracting the as-cleaved spectrum from the 0.8 L spectrum. An additional dose of 1.0 L at 120 K leads to a peak at 533.1 eV, indicative of multilayer water. The peak position was determined by subtracting the as-cleaved spectrum from the "+1.0 L at 120 K" spectrum. Supplementary Figure 9 shows the Sr *3d* region.

Spectra shown in Figure 4c were taken from a different sample and showed shifts of approximately 2 eV to higher binding energy. The shifts stayed constant over the course of the measurement. Most probably they were caused by insufficient electrical conductivity of the interface sample/epoxy glue and/or epoxy glue/sample plate. The shift was corrected by aligning all spectra to the higher binding energy peak of the two-peak structure, the binding energy of which is 529.4 eV as determined from the spectra shown in Supplementary Figure 7.

4.1 DFT core level calculations

The DFT calculations for the O*1s* core level energies of Sr_2RuO_4(001) were performed in the final state approximation. All calculations on bulk and slab cells were done using the Vienna Ab-Initio Simulation Package (VASP) employing

Site	Energy [eV]
O_A	0
O_P	0.89
low coverage OH	1.92
high coverage H_2O	3.68

Supplementary Table 4 | Calculated O*1s* core level shifts of Sr_2RuO_4(001). The apical oxygen atom O_A is situated at the rocksalt-like SrO interface and the planar O_P atoms in the RuO layer. Low coverage OH and high coverage H_2O denote adsorbed dissociated and molecular water, respectively.

PAW potentials and the optB86b functional including vdW interactions. For the bulk cell a $10 \times 10 \times 10$ Γ-centered k-point grid resulting in 126 irreducible k-points was used and for the slab calculations a $3 \times 3 \times 1$ Γ-centered k-point grid with 5 irreducible k-points. The energy cutoff for all calculations was 400 eV. For the bulk a $2 \times 2 \times 1$ unit cell with the lattice parameters a, b = 7.725 Å and c = 12.723 Å was used. The slab cell consists of a (4×4) Sr_2RuO_4(001) double layer with the lattice parameters a, b = 15.450 Å and 16.697 Å vacuum between the uppermost atom of the adsorbates and the lower side of the substrate slab.

The O*1s* core level shifts of adsorbed molecular (high coverage H_2O) and dissociated (low coverage OH) water are given with respect to the bulk O*1s* core levels. The O*1s* level of the bulk apical O atom at the rocksalt interface layer shows the lowest binding energy (O_A, see Supplementary Table 4) and is used as reference level. The O*1s* core levels of the O atoms in the RuO layer (O_P) shift by 0.890 eV to higher binding energies. At low H_2O coverage the O*1s* core level of the dissociated water molecule (OH) exhibits a shift of 1.920 eV with respect to O_A. Several models were investigated for the high coverage adsorption (0.5 ML) of the mixed dissociated and molecular H_2O phase. In a typical configuration as shown in Supplementary Figure 6, the O*1s* core level of undissociated molecular H_2O is found at a 3.680 eV higher binding energy.

References

[1] J. D. Wrigley, M. E. Twigg, and G. Ehrlich, "Lattice walks by long jumps," *The Journal of Chemical Physics*, vol. 93, no. 4, p. 2885, 1990.

[2] B. Stöger, M. Hieckel, F. Mittendorfer, Z. Wang, M. Schmid, G. S. Parkinson, D. Fobes, J. Peng, J. E. Ortmann, A. Limbeck, Z. Mao, J. Redinger, and U. Diebold, "Point defects at cleaved $Sr_{n+1}Ru_nO_{3n+1}(001)$ surfaces," *Phys. Rev. B*, vol. 90, p. 165438, 2014.